Time-Frequency Disentanglement Boosted Pre-Training: A Universal Spatio-Temporal Modeling Framework

Yudong Zhang[1,2] , **Zhaoyang Sun**[1] , **Xu Wang**[1,2*] , **Xuan Yu**[1] , **Kai Wang**[1] and **Yang Wang**[1,2,3*]

[1] University of Science and Technology of China (USTC), Hefei, China
[2] Suzhou Institute of Advanced Research, USTC, Suzhou, China
[3] State Key Laboratory of Precision and Intelligent Chemistry, USTC, Hefei, China
{zyd2020@mail., sunzhaoyang@mail., wx309@, yx2024@mail., zaizwk@mail., angyan@ }ustc.edu.cn

Abstract

Current spatio-temporal modeling techniques largely rely on the abundant data and the design of task-specific models. However, many cities lack well-established digital infrastructures, making data scarcity and the high cost of model development significant barriers to application deployment. Therefore, this work aims to enable spatio-temporal learning to cope with the problems of few-shot data modeling and model generalizability. To this end, we propose a <u>U</u>niversal <u>S</u>patio-<u>T</u>emporal <u>C</u>orrelationship pre-training framework (**USTC**), for spatio-temporal modeling across different cities and tasks. To enhance the spatio-temporal representations during pre-training, we propose to decouple the time-frequency patterns within data, and leverage contrastive learning to maintain the time-frequency consistency. To further improve the adaptability to downstream tasks, we design a prompt generation module to mine personalized spatio-temporal patterns on the target city, which can be integrated with the learned common spatio-temporal representations to collaboratively serve downstream tasks. Extensive experiments conducted on real-world datasets demonstrate that USTC significantly outperforms the advanced baselines in forecasting, imputation, and extrapolation across cities.

1 Introduction

Spatio-temporal graph learning is not only a powerful tool for understanding complex urban systems but also an intelligent measure for modeling the evolution of human behavior and natural environment [Shi *et al.*, 2023; Zhang *et al.*, 2024]. Despite the advances in spatio-temporal graph learning, most existing methods are typically designed for specific tasks and assume access to large volumes of high-quality data [Wang *et al.*, 2020; Liu *et al.*, 2025a; Miao *et al.*, 2024a; Liao *et al.*, 2024; Miao *et al.*, 2025]. However, this assumption often breaks down in numerous real-world urban environments, particularly in newly developed areas [Wang *et al.*, 2019; Deng *et al.*,

---

*Prof. Yang Wang and Dr. Xu Wang are the corresponding authors. Primary Contact: Dr. Xu Wang.

2024]. These areas frequently possess few or no pre-deployed sensors, making it difficult to collect sufficient data for training robust models. This dilemma makes us think about *how to carry out effective spatio-temporal graph few-shot learning in such data-scarce areas.* Furthermore, as smart applications become more ubiquitous, the demand for deploying diverse services continues to grow. Developing, training, and maintaining separate spatio-temporal models for each service or task is not only resource-intensive but also significantly slows down the deployment of intelligent urban solutions [Zhang *et al.*, 2023]. Therefore, *there is a pressing need for the generalization of spatio-temporal models enabling a universal model to adapt to different tasks with minimal retraining.*

As a promising cross-domain and cross-task knowledge transfer approach, transfer learning, dominated by pre-training techniques, aims to utilize the knowledge learned from data-rich sources domain to perform various downstream tasks in a data-scarce target domain [Zhuang *et al.*, 2020; Liu *et al.*, 2025b]. In recent years, researchers have realized the significant potential of pre-trained spatio-temporal models for cross-city few-shot learning and cross-task generalization, and have proposed a variety of solutions [Shao *et al.*, 2022; Jin *et al.*, 2023a]. For example, TPB [Liu *et al.*, 2023] utilizes a pre-trained traffic patch encoder to project raw traffic data from data-rich cities into a high-dimensional space. STGP [Hu *et al.*, 2024] proposes a prompt-enhanced transfer learning framework capable of adapting to diverse tasks in data-scarce domains. Existing pre-trained spatio-temporal models basically inherited the idea of Masked Autoencoder in STEP [Shao *et al.*, 2022] and achieved superior performance, but we deeply find that there are still two critical **challenges** that have not yet been adequately addressed, constraining the development of more universal spatio-temporal models.

Challenge 1. **Inadequate ability to represent spatio-temporal information in source domains.** The existing models are based on self-supervised learning methods in the time domain [Shao *et al.*, 2022], which neglects the complex and indispensable topological relationships in the spatial dimension in spatio-temporal data on the one hand, making the models lack the ability to model spatial information. On the other hand, just as important as the time domain are the temporal patterns in the frequency domain, whereas such potential but inherent trend information in spatio-temporal data has seldom been considered in spatio-temporal pre-training. Therefore,

these two shortcomings severely limit the effective extraction of spatio-temporal information from the source domains.

Challenge 2. **Deficient adaptability to target domains and tasks.** Most of the approaches add specific modules for different downstream tasks for training in the fine-tuning stage [Liu *et al.*, 2023]. This seemingly simple approach fails to pay attention to the individualized information of the graph structure in the target city on the one hand, leading to poor results even after fine-tuning the model, and on the other hand, it greatly reduces the model's generalizability and complicates the process of adapting the model to different tasks. Undoubtedly, improving the model's ability to adapt to target domains and downstream tasks will unleash the greater potential of pre-trained spatio-temporal models.

To effectively address the above challenges, we propose a **U**niversal **S**patio-**T**emporal **C**orrelationship pre-training framework (termed **USTC**), for spatio-temporal modeling across different cities and tasks. In particular, for *Challenge 1*, we decouple the time- and frequency-domain patterns of trend and seasonality in the data respectively during pre-training. After patched masking, we introduce a stacked structure of Transformer and Graph Neural Network (GNN) in encoding the spatio-temporal information and apply contrastive learning to the encoded time- and frequency-domain information to maintain the consistency of the original signals. For *Challenge 2*, we propose a prompt generation module in the fine-tuning stage to mine the personalized information in each node on the target city, which is combined with the shared spatio-temporal representations learned by the pre-trained encoder to serve the downstream tasks, and we introduce a common decoder for the three mainstream spatio-temporal tasks (*i.e.*, forecasting, imputation, and extrapolation) to extract the common semantics among the tasks and achieve cross-task generalization. The main **contributions** of our work lie in three aspects:

❶ *Novel insight and framework:* We innovatively construct a cross-city and cross-task spatio-temporal learning paradigm, and propose a time-frequency disentanglement boosted pre-training architecture called **USTC**, which enables the effective solution of spatio-temporal forecasting, imputation, and extrapolation with a universal model.

❷ *Advisable methodologies:* To enhance the spatio-temporal representations in pre-training, we decouple the time- and frequency-domain patterns of trend and seasonality in the data respectively, introduce the stacked structure of Transformer and GNN for spatio-temporal relationship extraction, and use contrastive learning for the encoded information to maintain the time-frequency consistency. To improve the adaptability of downstream tasks in fine-tuning, we propose a prompt generation module to mine personalized spatio-temporal patterns on the target city, which are integrated with the common spatio-temporal representations to collaboratively serve the downstream tasks.

❸ *Compelling empirical results:* We conduct extensive experiments on four real-world datasets, evaluating USTC on spatio-temporal forecasting, imputation, and extrapolation tasks. The results consistently demonstrate the superior performance of USTC across various scenarios.

2 Preliminaries

Definition 1. *Spatio-Temporal Graph.* *A spatio-temporal graph can be denoted as* $\mathcal{G} = (\mathcal{V}, \mathcal{E}, \mathbf{A})$ *[Fang* et al., *2023; Zhang* et al., *2025a; Zhang* et al., *2025b].* $\mathcal{V}$ *is the set of nodes,* $N = |\mathcal{V}|$ *is the number of nodes, and* $\mathcal{E}$ *is the set of edges.* $\mathbf{A} \in \mathbb{R}^{N \times N}$ *is the adjacency matrix of* $\mathcal{G}$, *which describes the weights between nodes.*

Definition 2. *Spatio-Temporal Data.* *Spatio-temporal data contained in the spatio-temporal graph can be denoted as* $\mathbf{X} \in \mathbb{R}^{N \times T \times C}$, *where* N *represents the number of nodes,* T *represents a time window, and* C *indicates the channel of inputs. And we donoted the spatio-temporal data of node* i *at time step* t *as* $\mathbf{X}_t^i \in \mathbb{R}^C$ *[Fang* et al., *2024].*

Problem 1. *Spatio-Temporal Graph Transfer Learning.* *Given* P *data-rich source domains* $\mathcal{G}^{source} = \{\mathcal{G}_1^{source}, \cdots, \mathcal{G}_P^{source}\}$ *and a data-scarce target domain* $\mathcal{G}^{target}$. *The goal of spatio-temporal graph transfer learning is to pre-train a model on the data of* $\mathcal{G}^{source}$ *to assimilate the relevant knowledge of the source domains, and fine-tune the model to adapt to the target domain* $\mathcal{G}^{target}$ *by utilizing the knowledge acquired. The fine-tuned model is required to accomplish various spatio-temporal graph learning tasks.*

Problem 2. *Forecasting.* *Given the historical spatio-temporal data of* T_h *time steps from a target domain, the goal of the forecasting problem is to transfer the pre-trained function* $f(\cdot)$ *to forecast the future data of* T_f *time steps [Liu* et al., *2024a; Miao* et al., *2024b]. This task can be formulated as follows:*

$$[\mathbf{X}_1, \cdots, \mathbf{X}_{T_h}] \xrightarrow{f(\cdot)} [\mathbf{X}_{T_h+1}, \cdots, \mathbf{X}_{T_h+T_f}], \quad (1)$$

where $\mathbf{X}_{[T_h+1:T_h+T_f]} \in \mathbb{R}^{N \times T_f \times C}$ *is the future data.*

Problem 3. *Imputation.* *Given incomplete historical data of* T_h *time steps from a target domain with missing values at certain time steps, the goal of imputation is to use the pre-trained function* $f(\cdot)$ *to estimate and fill in the missing data. To characterize the missing situation of time step* t, *we create a 0-1 matrix as* $\mathbf{R}_t \in \{r_{ij}\}_{i,j=1}^{N,C}$, *where* m_{ij} *is defined as:*

$$r_{ij} = \begin{cases} 0, & \text{if data is missing} \\ 1, & \text{otherwise} \end{cases}. \quad (2)$$

Therefore, the data with missing values of time step t *can be defined as* $\tilde{\mathbf{X}}_t = \mathbf{X}_t \odot \mathbf{R}_t$, *where* $\mathbf{X}_t$ *indicates the complete historical data of time step* t. *The problem of missing imputation can be formulated as follows:*

$$[\tilde{\mathbf{X}}_1, \cdots, \tilde{\mathbf{X}}_{T_h}] \xrightarrow{f(\cdot)} [\hat{\mathbf{X}}_1, \cdots, \hat{\mathbf{X}}_{T_h}], \quad (3)$$

where $\hat{\mathbf{X}}_{1:T_h} \in \mathbb{R}^{N \times T_h \times C}$ *represents the imputed data.*

Problem 4. *Extrapolation.* *Given the known historical spatio-temporal data of* T_h *time steps from* N *observed nodes within a target domain, the goal of the extrapolation task is to utilize this information to predict the future data of* T_f *time steps of* M *unobserved nodes [Zhang* et al., *2025c]. This task can be formulated as follows:*

$$\mathbf{X}_{1:T_h}^{1:N} \xrightarrow{f(\cdot)} \mathbf{X}_{T_h+1:T_h+T_f}^{N+1:N+M}, \quad (4)$$

where $\mathbf{X}_{T_h+1:T_h+T_f}^{N+1:N+M} \in \mathbb{R}^{M \times T_f \times C}$ *represents the future data of unobserved nodes.*
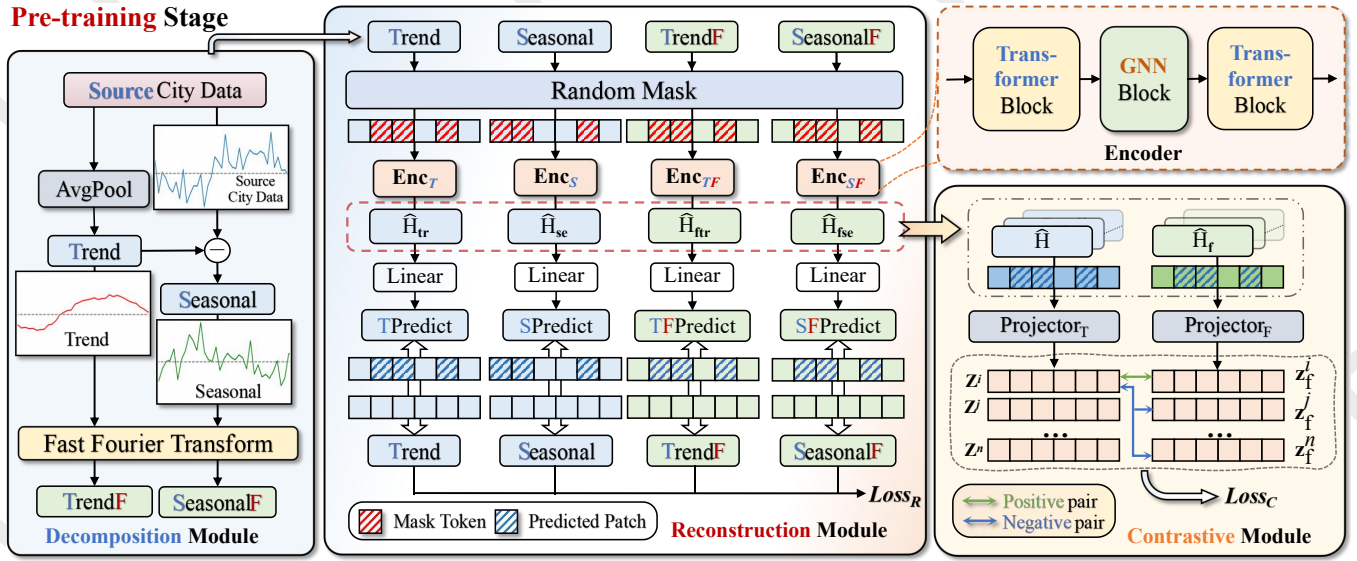
Figure 1: Overview of the pre-training stage in USTC, which consists of decomposition, reconstruction, and contrastive modules.

3 Methodology

In this section, we present an overview of the proposed USTC framework, which contains t**wo stages**:

Stage 1. *Pre-training*. *In this stage, we aim to learn robust knowledge from source domains. We introduce three novel modules as shown in Fig. 1. The first module is the **Decomposition Module**, which aims to process the source city data into four unique time-frequency information by leveraging average pooling and Fast Fourier Transform (FFT) techniques. The transformed information is then channeled as input into the subsequent **Reconstruction Module**. Within the **Reconstruction module**, inspired by [Shao et al., 2022; Liu et al., 2024c], we employ random masking and reconstruction strategies to learn the underlying temporal dynamics and spatial relationships. Furthermore, we introduce the **Contrastive Module** to encourage the encoder's capability to capture consistency across temporal and frequency domains.*

Stage 2. *Fine-tuning*. *The function of this stage is to adjust the model utilizing data from the target domain and task. Within this stage, the encoder, which was developed during the pre-training phase, is set to a fixed state. We have integrated a novel **Prompt Generation Module**, based on the consideration of node-specific knowledge that is ignored by the pre-trained encoder. To address this, we compute the difference between the encoder's input and output, and subsequently feed it into the prompt layer to generate node embeddings. These node embeddings are then concatenated with the hidden states extracted by the frozen encoder and introduced to the decoder. This approach enables the model to adapt to the distinct downstream tasks associated with the target city.*

3.1 Pre-Training Stage

Decomposition Module

Inspired by AutoFormer [Wu *et al.*, 2021a] and CoST [Woo *et al.*, 2022], we utilize the decomposition strategy to learn the intricate temporal patterns, which separate spatio-temporal data

into the trend and seasonal parts, which respectively reflect the long-term tendencies and the periodic seasonal variations inherent in the data. Specifically, we utilize the moving average to smooth out periodic fluctuations to yield the long-term trend component. Subsequently, by subtracting this trend component from the original data, we obtain the seasonal component. For the data $\mathbf{X}^i \in \mathbb{R}^{T \times C}$ of node i, the aforementioned decomposition operation can be represented as follows:

$$\begin{aligned} \mathbf{X}_{tr}^i &= \text{AvgPool}(\text{Padding}(\mathbf{X}^i)), \\ \mathbf{X}_{se}^i &= \mathbf{X}^i - \mathbf{X}_{tr}^i, \end{aligned} \quad (5)$$

where $\mathbf{X}_{tr}^i, \mathbf{X}_{se}^i \in \mathbb{R}^{T \times C}$ denote the trend component and the seasonal component of $\mathbf{X}^i$.

In addition, spatio-temporal data contains significant information in the frequency domain that is not evident in the time domain. To unearth this latent information, we employ the Fast Fourier Transform (FFT) to convert both trend and seasonal components into frequency domain, thereby capturing their spectral characteristics, which are delineated as follows:

$$\mathbf{F}_{tr}^i = \text{FFT}(\mathbf{X}_{tr}^i), \quad \mathbf{F}_{se}^i = \text{FFT}(\mathbf{X}_{se}^i), \quad (6)$$

where $\mathbf{F}_{tr}^i$ and $\mathbf{F}_{se}^i$ denote the frequency domain representations converted from $\mathbf{X}_{tr}^i$ and $\mathbf{X}_{se}^i$, respectively.

Through the decomposition module, we have decomposed and transformed the spatio-temporal data into four sets of time-frequency components, which are represented as $\mathbf{X}_{tr}^i$ and $\mathbf{X}_{se}^i$ in the time domain, and $\mathbf{F}_{tr}^i$ and $\mathbf{F}_{se}^i$ in the frequency domain.

Reconstruction Module

The reconstruction module is designed to leverage masking and reconstruction strategies for the pre-training of the encoder [Shao *et al.*, 2022]. Firstly, we perform random masking operations on the four sets of time-frequency data obtained from the decomposition module of the source cities. Formally, by taking the time domain as an example, we separate the input data of node i into P patches as $\mathbf{X}^i = \{\mathbf{S}_1^i, \ldots, \mathbf{S}_P^i\}$.

And we use a vector M to indicate whether a patch is masked or not, for example, $M_j^i = 1$ indicates $\mathbf{S}_j^i$ is masked. Then, the unmasked part of the input is fed into four distinct encoders, and a learnable masked token $\mathbf{S_{mt}}$ fills the place where the data is masked. Formally, the input can be denoted as:

$$\tilde{\mathbf{X}}^i = \text{Concatenate}\{\mathbf{S}_j^i, \mathbf{S_{mt}} \mid M_j^i = 0\}, \quad (7)$$

where $\tilde{\mathbf{X}}^i$ indicates the input sequence that has undergone the masking operation. Given that the structure of the four encoders is analogous, we will focus on trend data in the time domain as a representative example to explain. The encoder consists of three steps, each designed to process the input data and extract specific types of information. The initial step involves using a Transformer block, which is adept at capturing temporal dynamics within the input.

$$\mathbf{H}^i = \text{Transformer}_e(\tilde{\mathbf{X}}^i). \quad (8)$$

In the second step, a GNN block processes the relationships and interactions between different nodes, enabling the model to understand the spatial dependencies within the data.

$$\mathbf{H}^i = \text{GNN}_e(\mathbf{H}^j \mid j \in \mathcal{N}_i), \quad (9)$$

where $\mathcal{N}_i$ is the set of neighboring nodes of node i. Similar to the first step, the third step utilizes a Transformer block to refine the temporal features that have been extracted, which helps to consolidate the temporal patterns identified earlier and integrate any spatial insights gained from the GNN module.

$$\hat{\mathbf{H}}^i = \text{Transformer}_e'(\mathbf{H}^i), \quad \hat{\mathbf{X}}^i = W \cdot \hat{\mathbf{H}}^i + b. \quad (10)$$

Here $\hat{\mathbf{H}}^i$ denotes the output hidden embeddings of encoders, $\hat{\mathbf{X}}^i$ indicates the reconstructed sequence of node i. W and b represent the weight matrix and bias vector associated with the linear transformation applied after the Transformer block's processing. Therefore, we have the following formula:

$$\begin{aligned}
\hat{\mathbf{H}}_{\text{tr}}^i &= \text{Enc}_T\left(\tilde{\mathbf{X}}_{\text{tr}}^i\right), & \hat{\mathbf{X}}_{\text{tr}}^i &= \text{Linear}\left(\hat{\mathbf{H}}_{\text{tr}}^i\right), \\
\hat{\mathbf{H}}_{\text{se}}^i &= \text{Enc}_S\left(\tilde{\mathbf{X}}_{\text{se}}^i\right), & \hat{\mathbf{X}}_{\text{se}}^i &= \text{Linear}\left(\hat{\mathbf{H}}_{\text{se}}^i\right), \\
\hat{\mathbf{H}}_{\text{ftr}}^i &= \text{Enc}_{TF}\left(\tilde{\mathbf{F}}_{\text{tr}}^i\right), & \hat{\mathbf{X}}_{\text{ftr}}^i &= \text{Linear}\left(\hat{\mathbf{H}}_{\text{ftr}}^i\right), \\
\hat{\mathbf{H}}_{\text{fse}}^i &= \text{Enc}_{SF}\left(\tilde{\mathbf{F}}_{\text{se}}^i\right), & \hat{\mathbf{X}}_{\text{fse}}^i &= \text{Linear}\left(\hat{\mathbf{H}}_{\text{fse}}^i\right).
\end{aligned} \quad (11)$$

Then, the reconstruction loss can be formulated as follows:

$$\begin{aligned}
\mathcal{L}_{\text{R}} = &\sum_{i=1}^{N}\sum_{j=1}^{P} M_{\text{tr},j}^i \left(\mathbf{S}_{\text{tr},j}^i - \hat{\mathbf{S}}_{\text{tr},j}^i\right)^2 \\
&+ \sum_{i=1}^{N}\sum_{j=1}^{P} M_{\text{se},j}^i \left(\mathbf{S}_{\text{se},j}^i - \hat{\mathbf{S}}_{\text{se},j}^i\right)^2 \\
&+ \sum_{i=1}^{N}\sum_{j=1}^{P} M_{\text{ftr},j}^i \left(\mathbf{S}_{\text{ftr},j}^i - \hat{\mathbf{S}}_{\text{ftr},j}^i\right)^2 \\
&+ \sum_{i=1}^{N}\sum_{j=1}^{P} M_{\text{fse},j}^i \left(\mathbf{S}_{\text{fse},j}^i - \hat{\mathbf{S}}_{\text{fse},j}^i\right)^2.
\end{aligned} \quad (12)$$

We encourage the encoders to harness the intrinsic information within the time-frequency data by optimizing their parameters to minimize the reconstruction loss, enhancing the encoders' capacity to accurately reconstruct the partially masked input.

Contrastive Module

We introduce a contrastive module to reinforce time-frequency consistency within the data, which refers to the notion that the characteristics of a signal in the time domain should correspond to those in the frequency domain [Liu *et al.*, 2024b; Zhang *et al.*, 2022]. Here, we focus on the time-frequency consistency rather than the differences between trend and seasonal data. Therefore, we omit the subscripts $_{\text{tr}}$ and $_{\text{se}}$ and use $\hat{\mathbf{H}}$ to denote the time-domain hidden embeddings output by the encoders, and $\hat{\mathbf{H}}_{\text{f}}$ to represent the frequency-domain hidden embeddings. To ensure the measurability of the distance between time- and frequency-domain embeddings, we project the time- and frequency-domain embeddings through two distinct projection operators, $\text{Projector}_{\text{T}}$ and $\text{Projector}_{\text{F}}$, respectively. The formulation can be articulated as follows:

$$\mathbf{Z} = \text{Projector}_{\text{T}}(\hat{\mathbf{H}}), \quad \mathbf{Z}_{\text{f}} = \text{Projector}_{\text{F}}(\hat{\mathbf{H}}_{\text{f}}). \quad (13)$$

To maintain a set of time-domain data more similar to its corresponding frequency-domain data obtained through FFT, we use the NT-Xent Loss [Chen *et al.*, 2020] to optimize the encoders, which can be formulated as:

$$\mathcal{L}_{\text{C}} = -\sum_{i}^{N} \log \frac{e^{\text{sim}(\mathbf{Z}^i, \mathbf{Z}_{\text{f}}^i)}}{\sum_j e^{\text{sim}(\mathbf{Z}^i, \mathbf{Z}_{\text{f}}^j)}}, \quad (14)$$

where sim indicates the cosine similarity, and the negative samples $\mathbf{Z}_{\text{f}}^j$ are chosen from N nodes randomly. This approach encourages the model to preserve the consistency between time- and frequency-domain embeddings. The total loss $\mathcal{L}_P$ of pre-training stage is the weighted sum of $\mathcal{L}_{\text{R}}$ and $\mathcal{L}_{\text{C}}$.

$$\mathcal{L}_P = \mathcal{L}_{\text{R}} + \alpha\mathcal{L}_{\text{C}}, \quad (15)$$

where α is a regularization weight for balancing this combined loss. Thus, the model is optimized to achieve time-frequency consistency while learning diverse representations.

3.2 Fine-Tuning Stage

Prompt Generate Module

The prompt generation module is designed to obtain node embeddings that capture the personalized information ignored by the encoders. We calculate the difference between the target city's data and the output derived from processing this data through the encoders, thereby identifying the information that the encoders have potentially missed. This information is then passed into the Prompt Layer to obtain the node embedding $\mathbf{P}^i$. Formally, this process can be articulated as follows:

$$\hat{\mathbf{H}}_{\text{total}}^i = \hat{\mathbf{H}}_{\text{tr}}^i + \hat{\mathbf{H}}_{\text{se}}^i + \text{IFFT}\left(\hat{\mathbf{H}}_{\text{ftr}}^i\right) + \text{IFFT}\left(\hat{\mathbf{H}}_{\text{fse}}^i\right),$$

$$\mathbf{P}^i = \text{PromptLayer}\left(\mathbf{X}^i - W_P \cdot \hat{\mathbf{H}}_{\text{total}}^i\right), \quad (16)$$

where IFFT is the Inverse Fast Fourier Transform. We hypothesize that the Euclidean distance between the node embeddings should correlate with the distances reflected by Dynamic Time Warping (DTW) [Berndt and Clifford, 1994]. To represent this similarity, we employ a Mean Squared Error (MSE) Loss, with the specific formula provided as follows:

$$\mathcal{L}_{pro} = \frac{1}{n(n-1)} \sum_{i=1}^{n} \sum_{j=1, j \neq i}^{n} (D_{\text{DTW}}(\mathbf{X}^i, \mathbf{X}^j) - D_{\text{Euc}}(\mathbf{P}^i, \mathbf{P}^j))^2, \quad (17)$$
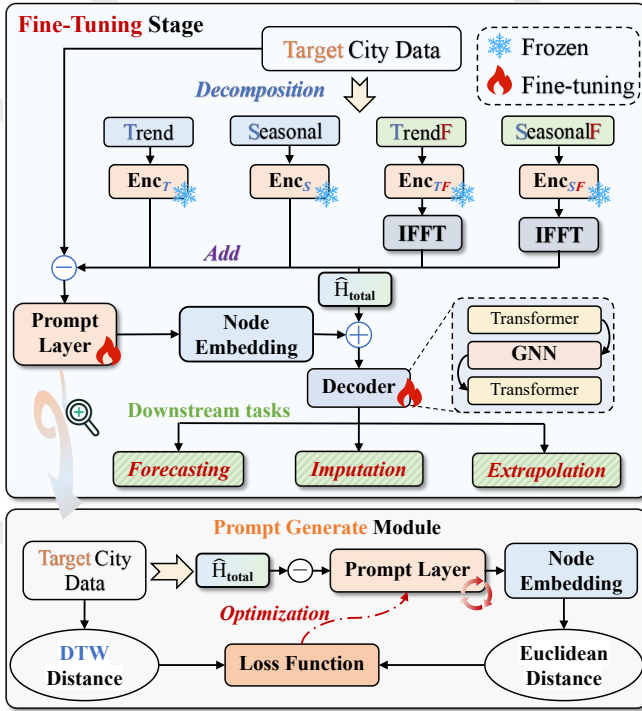
Figure 2: Overview of the fine-tuning stage in USTC.

where D_{DTW} is DTW distance between two time sequences, D_{Euc} ies Euclidean distance between encoded embeddings, and n is the number of nodes in the target city. The fine-tuning of the prompt layer is guided by minimizing this loss, thereby ensuring that the node embeddings closely reflect the fine-grained personalized features of the target domain.

Fine-Tuning Module
In fine-tuning, our goal is to align the pre-trained encoders with the distinctive attributes of the target city. As illustrated in Fig. 2, we keep the encoders fixed while fine-tuning the prompt layer and decoder. The node embeddings $\mathbf{P}$ generated in the prompt generation module are concatenated with the hidden states $\hat{\mathbf{H}}_{\text{total}}$ and then passed into the decoder. Echoing the encoders, the decoder also adopts a stacked structure to decouple the learned spatio-temporal representations. Formally:

$$\hat{\mathbf{H}}^i = \text{Decoder}\left(\text{Concatenate}\{\hat{\mathbf{H}}^i_{\text{total}}, \mathbf{P}^i\}\right),$$
$$\hat{y}^i = \text{Linear}\left(\hat{\mathbf{H}}^i\right). \tag{18}$$

MSE loss is utilized to optimize the decoder and prompt layer,

$$\mathcal{L}_{task} = \frac{1}{nT_fC}\sum_{i=1}^{n}\sum_{j=1}^{T_f}\sum_{k=1}^{C}\left(y_{ijk} - \hat{y}_{ijk}\right)^2. \tag{19}$$

Finally, the total loss $\mathcal{L}_F$ in fine-tuning is formalized as,

$$\mathcal{L}_F = \mathcal{L}_{task} + \beta\mathcal{L}_{pro}. \tag{20}$$

This fine-tuning procedure guarantees that the model can adeptly perform diverse downstream tasks within the target city, encompassing forecasting, imputation, and extrapolation.

Datasets	PEMS-BAY	METR-LA	Chengdu	Shenzhen
# of Nodes	325	207	524	627
# of Edges	2,694	1,722	1,120	4,845
Interval	5 min	5 min	10 min	10 min
# of Time Step	52,116	34,272	17,280	17,280
Mean	61.7768	58.2749	29.0235	31.0092
Std	9.2852	13.1280	9.6620	10.9694

Table 1: Statistical details of traffic datasets.

4 Experiments

4.1 Experimental Setup

Datasets. Four real-world widely used datasets are employed to evaluate our proposed framework, including *PEMS-BAY*, *METR-LA* [Li *et al.*, 2018], *Chengdu*, and *Shenzhen*. These datasets comprise several months of traffic flow information, with the statistics listed in Table 1.

Few-Shot Transfer Learning Setting. Our framework is evaluated using a few-shot fine-tuning setting that aligns with [Lu *et al.*, 2022; Liu *et al.*, 2023]. The dataset is divided into three parts: pre-training data from three cities, few-shot fine-tuning data, and testing data from the other city. We use the comprehensive data from three cities for pre-training and select one city's data for both few-shot fine-tuning and testing. For instance, if *Shenzhen* is the city chosen for fine-tuning, the complete datasets from *PEMS-BAY*, *METR-LA*, and *Chengdu* are used for pre-training. A three-day dataset from *Shenzhen* is allocated for few-shot fine-tuning, while the rest of the data in *Shenzhen* is reserved for testing. We consider three classic tasks, including: 1) *forecasting*, predicting the future 1-hour data based on 1-day historical data. 2) *imputation*, forecasting the missing values within a given time window. 3) *extrapolation*, forecasting the future data of unobserved nodes, whose historical data is unknown. We use two widely used regression metrics: Mean Absolute Error (MAE) and Root Mean Squared Error (RMSE).

Baselines. We compare our model with 18 baseline models across three categories, which are listed as follows,
❶ **Statistical Methods:** HA and ARIMA calculate the statistical properties of input data to predict future signals. MEAN calculates the average value of the input and uses it to complete missing data. KNN completes missing data with the average value of its neighbors.
❷ **Typical Deep-learning Methods:** DCRNN [Li *et al.*, 2018], ICREASE [Zheng *et al.*, 2023], GWN [Wu *et al.*, 2019], DSTAGNN [Lan *et al.*, 2022], and FOGS [Rao *et al.*, 2022] are classical models for spatiotemporal prediction. To apply them in the transfer learning scenario, we optimize them using the *Reptile* [Nichol *et al.*, 2018] meta-learning framework.
❸ **Transfer-learning Models:** AdaRNN [Du *et al.*, 2021], ST-GFSL [Lu *et al.*, 2022], DASTNet [Tang *et al.*, 2022], TPB [Liu *et al.*, 2023], IGNNK [Wu *et al.*, 2021b], SATCN [Wu *et al.*, 2021c], TransGTR [Jin *et al.*, 2023b], GPD [Yuan *et al.*, 2024], and STGP [Hu *et al.*, 2024] represent the cutting-edge in time series or spatio-temporal forecasting within the domain of transfer learning.

Notably, the conventional deep-learning methods are implemented with *Reptile* framework, which is a meta-learning

Model	Target City	METR-LA								PEMS-BAY							
	Metrics	MAE(↓)				RMSE(↓)				MAE(↓)				RMSE(↓)			
	Horizon	10 min	30 min	60 min	avg.	10 min	30 min	60 min	avg.	10 min	30 min	60 min	avg.	10 min	30 min	60 min	avg.
HA	Target Only	3.62	4.23	5.13	4.33	7.33	8.56	10.17	8.69	2.42	2.89	3.70	3.00	5.46	6.52	8.25	6.74
ARIMA		3.22	3.70	5.00	3.97	6.28	7.80	9.80	7.96	2.28	2.49	3.66	2.81	4.52	5.35	7.45	5.77
DCRNN	Reptile	3.01	3.65	4.67	3.78	5.62	7.16	8.96	7.25	1.83	2.43	3.36	2.54	3.36	4.71	6.59	4.89
GWN		3.11	3.75	4.73	3.86	5.87	7.31	9.10	7.43	1.99	2.45	3.14	2.53	3.55	4.64	6.23	4.81
DSTAGNN		3.30	4.10	4.95	4.12	5.90	7.73	9.56	7.73	1.85	2.51	3.59	2.65	3.41	4.79	6.66	4.95
FOGS		3.26	4.11	4.88	4.08	5.95	7.50	9.47	7.64	1.89	2.38	3.37	2.55	3.49	4.54	6.01	4.68
AdaRNN	Transfer	3.05	3.68	4.51	3.75	5.66	7.15	8.60	7.14	1.79	2.33	3.04	2.39	3.38	4.60	5.98	4.65
ST-GFSL		3.00	3.79	4.58	3.79	5.72	7.21	8.67	7.20	1.77	2.20	2.95	2.31	3.27	4.50	5.92	4.56
DSATNet		3.03	3.66	4.51	3.73	5.70	7.15	8.78	7.21	1.64	2.16	2.88	2.23	3.26	4.36	5.89	4.50
TPB		3.07	3.80	4.66	3.84	5.69	7.03	8.52	7.08	1.62	2.12	2.83	2.19	3.24	4.33	5.76	4.44
TransGTR		3.01	3.64	4.44	3.70	5.60	7.12	8.49	7.07	**1.60**	2.13	2.79	2.17	**3.04**	4.35	5.68	4.36
GPD		2.96	3.58	4.29	3.61	5.58	6.90	8.21	6.90	1.72	2.18	2.69	2.20	3.19	4.26	5.60	4.35
STGP		2.97	3.54	4.23	3.58	5.48	6.77	8.19	6.81	1.74	2.13	2.70	2.19	3.21	4.18	5.46	4.28
USTC	Transfer	**2.85**	**3.41**	**4.10**	**3.45**	**5.37**	**6.58**	**8.10**	**6.68**	1.69	**2.05**	**2.63**	**2.12**	3.09	4.22	5.48	**4.26**

Model	Target City	Chengdu Dataset								Shenzhen Dataset							
	Metrics	MAE(↓)				RMSE(↓)				MAE(↓)				RMSE(↓)			
	Horizon	10 min	30 min	60 min	avg.	10 min	30 min	60 min	avg.	10 min	30 min	60 min	avg.	10 min	30 min	60 min	avg.
HA	Target Only	2.69	3.13	3.65	3.16	3.69	4.57	5.27	4.51	2.17	2.66	3.04	2.62	3.33	4.05	4.63	4.00
ARIMA		2.97	3.28	4.32	3.52	3.78	4.64	5.51	4.64	2.35	2.99	3.60	2.98	4.32	4.73	5.58	4.88
DCRNN	Reptile	2.31	3.16	3.96	3.14	3.33	4.55	5.42	4.43	1.94	2.57	3.07	2.53	2.84	3.81	4.52	3.72
GWN		2.19	2.81	3.21	2.74	3.12	4.08	4.65	3.95	1.88	2.46	2.82	2.39	2.77	3.68	4.26	3.57
DSTAGNN		2.36	3.01	3.40	2.92	3.21	4.20	4.97	4.13	1.98	2.43	2.95	2.45	2.90	3.69	4.27	3.62
FOGS		2.23	2.80	3.31	2.78	3.18	4.30	4.77	4.08	1.96	2.36	2.80	2.37	2.88	3.61	4.35	3.61
AdaRNN	Transfer	2.18	2.91	3.40	2.83	3.09	3.97	4.82	3.96	1.92	2.48	2.88	2.43	2.85	3.63	4.26	3.58
ST-GFSL		2.10	2.80	3.35	2.75	3.02	3.88	4.60	3.83	1.90	2.36	2.71	2.32	2.70	3.53	4.19	3.47
DSATNet		2.06	2.70	3.03	2.60	3.02	4.01	4.53	3.85	1.86	2.34	2.64	2.28	2.73	3.51	4.00	3.41
TPB		2.08	2.63	3.02	2.58	2.98	3.84	4.34	3.72	1.85	2.32	2.61	2.26	2.70	3.45	3.91	3.35
TransGTR		2.05	2.65	2.80	2.50	2.95	3.82	4.26	3.68	1.89	**2.30**	2.47	2.22	2.69	3.49	3.79	3.32
GPD		2.02	2.58	2.79	2.46	2.90	3.81	4.19	3.63	1.86	2.31	2.52	2.23	2.71	3.34	3.82	3.29
STGP		1.98	2.54	2.74	2.42	2.85	3.72	4.02	3.53	1.82	**2.27**	**2.42**	**2.17**	2.66	3.39	3.69	3.25
USTC	Transfer	**1.90**	**2.41**	**2.64**	**2.31**	**2.81**	**3.68**	**3.99**	**3.49**	**1.80**	2.34	2.48	2.21	**2.55**	**3.33**	**3.61**	**3.16**

Table 2: Forecasting performance comparison of few-shot learning on four spatio-temporal datasets. The best result is indicated in **bold** with light blue and the second-best result is with light gray , hereinafter the same.

approach as described by [Nichol *et al.*, 2018]. Since these baselines are not compatible with all three downstream tasks, we compare different baseline models for different tasks.

4.2 Performance Evaluation

❶ *Forecasting.* When the downstream task is forecasting, we use 1-day historical data to predict future 1-hour data, and the results are shown in Table 2. We can find that transfer learning methods achieve the best performance among all three categories of methods, underscoring the substantial potential of transfer learning in addressing few-shot challenges. Taking advantage of transfer learning, **our proposed USTC surpasses existing baselines across nearly all metrics and datasets**. Given that we compare USTC with seven transfer learning baselines, the performance gains are attributed to our distinctive designs, which are further assessed in the following.

❷ *Imputation.* In the imputation task, we predict the missing values in data among a time window of 25 hours. The missing values are generated by randomly masking observed data with a ratio of 30%. We examine two scenarios: transductive and inductive. In the transductive scenario, the model is trained with the full dataset available. In contrast, the inductive scenario poses a greater challenge as the model is pre-trained on incomplete data and does not have access to the masked values during training. The results are detailed in Table 3. Since the previous baselines are not suitable for imputation, we have

chosen different baselines for comparison. **The proposed USTC surpasses all baselines across all metrics, indicating a more significant advantage than in the forecasting task.** This superiority is attributed to that the imputation task is closer aligned with our pre-training, thus reducing the gap between pre-training and fine-tuning. Additionally, the imputation task is inherently more difficult due to the large missing data ratio we set, which explains the higher absolute MAE and RMSE values compared to those in the forecasting task.

❸ *Extrapolation.* In the extrapolation task, we mask 30% of the nodes from the complete data, designating them as unobserved nodes. Our objective is to predict the future 1-hour data for these unobserved nodes using a 1-day historical dataset of the observed nodes. Similarly, we evaluate this task under two scenarios: transductive and inductive. In the transductive scenario, the model is trained on the full dataset with all nodes available. In the inductive scenario, the model is trained on incomplete data and does not have access to the masked nodes during training. The results are reported in Table 3. Also, we compare our method with exclusive baselines for the extrapolation task. The proposed USTC method surpasses all baselines across all metrics. **This consistent outperformance across the three downstream tasks substantially validates the effectiveness of our framework.**

Model	Target City Metrics Setting	METR-LA MAE		RMSE		PEMS-BAY MAE		RMSE		Chengdu MAE		RMSE		Shenzhen MAE		RMSE	
		Trdu.	Indu.	Trdu.	Indu.	Trdu.	Indu.	Trdu.	Indu.	Trdu.	Indu.	Trdu.	Indu.	Trdu.	Indu.	Trdu.	Indu.
MEAN	Target Only	10.28		14.86		5.49		9.28		7.42		9.78		8.81		11.08	
KNN		9.11		12.88		4.2		7.55		7.01		9.4		8.89		11.17	
KCN	Reptile	5.64	7.75	8.70	11.75	3.89	4.72	6.86	8.19	6.60	7.00	8.95	9.28	5.68	8.25	8.04	10.94
IGNNK		5.66	7.56	9.32	11.65	3.89	4.28	7.14	7.17	6.68	7.52	8.88	9.89	5.39	8.16	7.55	10.89
SATCN		4.80	7.49	7.83	11.57	3.45	3.84	6.49	6.79	6.57	7.09	9.00	9.39	5.50	8.11	7.86	10.82
DualSTN		5.59	7.09	9.57	11.45	3.53	3.71	6.80	6.74	5.94	6.37	8.05	8.66	5.34	8.17	7.61	10.89
INCREASE		4.99	7.34	8.22	11.49	3.41	3.68	6.38	6.77	6.13	6.62	8.49	8.78	5.33	8.14	7.60	10.82
STGP	Transfer	4.50	6.94	7.72	11.37	3.36	3.64	6.27	6.64	5.43	6.29	7.65	8.63	5.23	8.07	7.45	10.75
USTC	Transfer	**4.29**	**6.46**	**7.26**	**11.21**	**3.27**	**3.55**	**6.20**	**6.58**	**4.99**	**6.17**	**7.49**	**8.48**	**5.15**	**7.82**	**7.35**	**10.47**

Table 3: Imputation performance of transfer learning on the datasets. Trdu./Indu. denote transductive/inductive settings.

Model	Target City Metrics Setting	METR-LA MAE		RMSE		PEMS-BAY MAE		RMSE		Chengdu MAE		RMSE		Shenzhen MAE		RMSE	
		Trdu.	Indu.	Trdu.	Indu.	Trdu.	Indu.	Trdu.	Indu.	Trdu.	Indu.	Trdu.	Indu.	Trdu.	Indu.	Trdu.	Indu.
MEAN	Target Only	10.64		15.27		5.56		9.31		7.53		9.74		8.91		11.63	
GWN	Reptile	5.41	9.26	9.69	15.10	4.32	5.01	8.09	9.86	5.83	7.21	8.25	9.61	4.02	8.47	5.74	11.40
DCRNN		5.10	9.41	9.19	15.57	3.64	5.12	6.97	10.14	6.23	7.10	8.62	9.58	3.85	8.64	5.31	11.54
IGNNK		6.67	9.14	10.33	14.63	3.90	5.05	7.13	9.90	6.52	7.43	8.81	9.71	4.41	8.52	6.47	11.38
SATCN		7.29	9.13	12.41	14.88	4.65	5.13	9.04	10.13	7.09	7.20	9.51	9.66	4.87	8.70	7.15	11.58
ST-GFSL	Transfer	7.73	9.31	12.31	14.99	4.27	4.59	7.61	7.92	6.51	6.79	8.74	9.41	4.75	8.55	6.99	11.45
TPB		7.97	9.01	12.50	14.42	4.40	4.53	7.79	7.83	6.12	6.67	8.37	9.27	4.66	8.38	6.96	11.23
TransGTR		7.33	8.87	11.22	14.12	4.55	4.66	7.95	8.10	6.42	6.62	8.65	9.10	4.58	8.45	6.81	11.36
STGP		5.04	8.51	9.03	13.49	3.41	4.13	6.47	7.52	5.46	6.51	7.67	8.91	3.61	8.22	5.04	11.07
USTC	Transfer	**4.82**	**8.19**	**8.94**	**13.21**	**3.18**	**3.99**	**6.17**	**7.28**	**5.26**	**6.33**	**7.48**	**8.74**	**3.44**	**8.09**	**4.96**	**10.82**

Table 4: Extrapolation performance of transfer learning on the datasets. The results are averaged over all 12 future horizons.

4.3 Ablation Study

To deeply analyze the effect of different components in USTC, we design six variants of our model: 1) *w/o trend*, removing trend components from the framework; 2) *w/o sea*, removing seasonal components; 3) *w/o time*, removing time-domain signals; 4) *w/o spec*, removing frequency-domain signals; 5) *w/o cons*, removing the contrastive learning module from pre-training; 6) *w/o prompt*, removing the prompt module from fine-tuning. We report the MAE on the four datasets regarding all tasks of all variants and USTC in Fig. 4. As shown, the prompt module in fine-tuning state contributes a lot to our framework. The contrastive module in the pre-training stage has a contribution similar to but slightly less than the prompt module. Additionally, the involvement of both time- and frequency-domain signals results in ignorable performance improvement. Overall, all the proposed novel components have a positive impact on the improvement of our framework.

4.4 Impact of Pre-training Datasets

We further investigate the impact of varying pre-training datasets and assess the robustness of different methods. STGP is compared due to its significant performance. As shown in Fig. 3, when the number of source cities is reduced, the volume of training data correspondingly decreases, leading to a performance decline in both models. However, our USTC, which leverages several designed components in pre-training, experiences less degradation. This outcome underscores the robustness of USTC with limited data for pre-training.
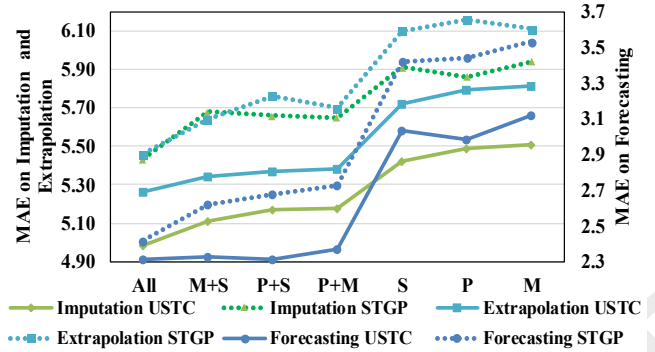

Figure 3: Impact of different pre-training datasets.

5 Conclusion

In this paper, we propose a novel universal spatio-temporal modeling framework (**USTC**) generalized to various cities and tasks. To enhance the spatio-temporal representations during pre-training, we decouple the time-frequency patterns within the data and employ contrastive learning to preserve time-frequency consistency. Furthermore, we design a prompt generation module to extract personalized spatio-temporal patterns from the target city, which can be integrated with the learned common representations to collaboratively support downstream tasks. Extensive experiments validate the effectiveness of USTC in three downstream tasks across cities.
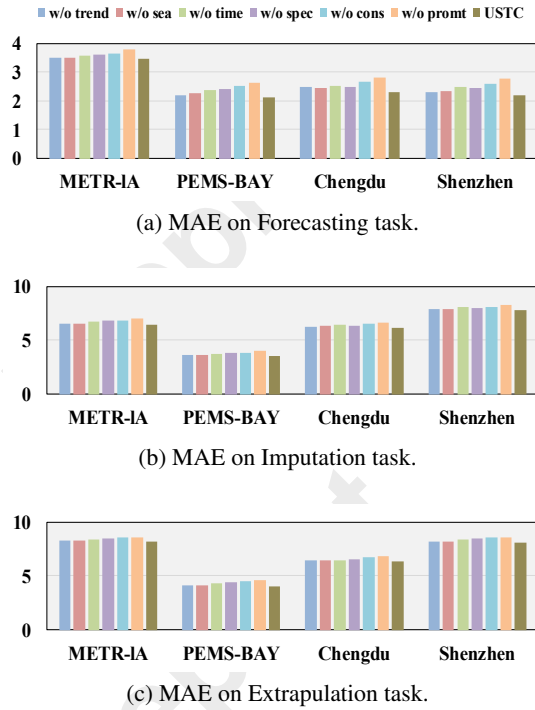
(a) MAE on Forecasting task.

(b) MAE on Imputation task.

(c) MAE on Extrapulation task.

Figure 4: Impact of different components in USTC.

Acknowledgments

References

[Berndt and Clifford, 1994] Donald J Berndt and James Clifford. Using dynamic time warping to find patterns in time series. In *Proceedings of the 3rd international conference on knowledge discovery and data mining*, pages 359–370, 1994.

[Chen *et al.*, 2020] Ting Chen, Simon Kornblith, Mohammad Norouzi, and Geoffrey Hinton. A simple framework for contrastive learning of visual representations. In *International conference on machine learning*, pages 1597–1607. PMLR, 2020.

[Deng *et al.*, 2024] Liwei Deng, Yan Zhao, Jin Chen, Shuncheng Liu, Yuyang Xia, and Kai Zheng. Learning to hash for trajectory similarity computation and search. In *2024 IEEE 40th International Conference on Data Engineering (ICDE)*, pages 4491–4503. IEEE, 2024.

[Du *et al.*, 2021] Yuntao Du, Jindong Wang, Wenjie Feng, Sinno Pan, Tao Qin, Renjun Xu, and Chongjun Wang. Adarnn: Adaptive learning and forecasting of time series. In *Proceedings of the 30th ACM international conference on information & knowledge management*, pages 402–411, 2021.

[Fang *et al.*, 2023] Yuchen Fang, Yanjun Qin, Haiyong Luo, Fang Zhao, Bingbing Xu, Liang Zeng, and Chenxing Wang. When spatio-temporal meet wavelets: Disentangled traffic forecasting via efficient spectral graph attention networks. In *2023 IEEE 39th International Conference on Data Engineering (ICDE)*, pages 517–529. IEEE, 2023.

[Fang *et al.*, 2024] Yuchen Fang, Yuxuan Liang, Bo Hui, Zezhi Shao, Liwei Deng, Xu Liu, Xinke Jiang, and Kai Zheng. Efficient large-scale traffic forecasting with transformers: A spatial data management perspective. *arXiv preprint arXiv:2412.09972*, 2024.

[Hu *et al.*, 2024] Junfeng Hu, Xu Liu, Zhencheng Fan, Yifang Yin, Shili Xiang, Savitha Ramasamy, and Roger Zimmermann. Prompt-enhanced spatio-temporal graph transfer learning. *arXiv preprint arXiv:2405.12452*, 2024.

[Jin *et al.*, 2023a] Ming Jin, Qingsong Wen, Yuxuan Liang, Chaoli Zhang, Siqiao Xue, Xue Wang, James Zhang, Yi Wang, Haifeng Chen, Xiaoli Li, et al. Large models for time series and spatio-temporal data: A survey and outlook. *arXiv preprint arXiv:2310.10196*, 2023.

[Jin *et al.*, 2023b] Yilun Jin, Kai Chen, and Qiang Yang. Transferable graph structure learning for graph-based traffic forecasting across cities. In *Proceedings of the 29th ACM SIGKDD Conference on Knowledge Discovery and Data Mining*, pages 1032–1043, 2023.

[Lan *et al.*, 2022] Shiyong Lan, Yitong Ma, Weikang Huang, Wenwu Wang, Hongyu Yang, and Pyang Li. Dstagnn: Dynamic spatial-temporal aware graph neural network for traffic flow forecasting. In *International conference on machine learning*, pages 11906–11917. PMLR, 2022.

[Li *et al.*, 2018] Yaguang Li, Rose Yu, Cyrus Shahabi, and Yan Liu. Diffusion convolutional recurrent neural network: Data-driven traffic forecasting. In *International Conference on Learning Representations*, 2018.

[Liao *et al.*, 2024] Tianchi Liao, Lele Fu, Jialong Chen, Zhen Wang, Zibin Zheng, and Chuan Chen. A swiss army knife for heterogeneous federated learning: Flexible coupling via trace norm. *Advances in Neural Information Processing Systems*, 37:139886–139911, 2024.

[Liu *et al.*, 2023] Zhanyu Liu, Guanjie Zheng, and Yanwei Yu. Cross-city few-shot traffic forecasting via traffic pattern bank. In *Proceedings of the 32nd ACM International Conference on Information and Knowledge Management*, pages 1451–1460, 2023.

[Liu *et al.*, 2024a] Chenxi Liu, Sun Yang, Qianxiong Xu, Zhishuai Li, Cheng Long, Ziyue Li, and Rui Zhao. Spatial-temporal large language model for traffic prediction. In *25th IEEE International Conference on Mobile Data Management*, pages 31–40, 2024.

[Liu *et al.*, 2024b] Zhanyu Liu, Jianrong Ding, and Guanjie Zheng. Frequency enhanced pre-training for cross-city few-shot traffic forecasting. In *Joint European Conference on Machine Learning and Knowledge Discovery in Databases*, pages 35–52. Springer, 2024.

[Liu *et al.*, 2024c] Zhanyu Liu, Guanjie Zheng, and Yanwei Yu. Multi-scale traffic pattern bank for cross-city few-shot traffic forecasting. *arXiv preprint arXiv:2402.00397*, 2024.

[Liu *et al.*, 2025a] Chenxi Liu, Hao Miao, Qianxiong Xu, Shaowen Zhou, Cheng Long, Yan Zhao, Ziyue Li, and Rui Zhao. Efficient multivariate time series forecasting via calibrated language models with privileged knowledge distillation. In *41th IEEE International Conference on Data Engineering*, 2025.

[Liu *et al.*, 2025b] Chenxi Liu, Shaowen Zhou, Qianxiong Xu, Hao Miao, Cheng Long, Ziyue Li, and Rui Zhao. Towards cross-modality modeling for time series analytics: A survey in the llm era. In *IJCAI*, pages 1–9, 2025.

[Lu *et al.*, 2022] Bin Lu, Xiaoying Gan, Weinan Zhang, Huaxiu Yao, Luoyi Fu, and Xinbing Wang. Spatio-temporal graph few-shot learning with cross-city knowledge transfer. In *Proceedings of the 28th ACM SIGKDD Conference on Knowledge Discovery and Data Mining*, pages 1162–1172, 2022.

[Miao *et al.*, 2024a] Hao Miao, Ziqiao Liu, Yan Zhao, Chenjuan Guo, Bin Yang, Kai Zheng, and Christian S Jensen. Less is more: Efficient time series dataset condensation via two-fold modal matching. *PVLDB*, 18(2):226–238, 2024.

[Miao *et al.*, 2024b] Hao Miao, Yan Zhao, Chenjuan Guo, Bin Yang, Kai Zheng, Feiteng Huang, Jiandong Xie, and Christian S Jensen. A unified replay-based continuous learning framework for spatio-temporal prediction on streaming data. In *ICDE*, pages 1050–1062, 2024.

[Miao *et al.*, 2025] Hao Miao, Ronghui Xu, Yan Zhao, Senzhang Wang, Jianxin Wang, Philip S Yu, and Christian S Jensen. A parameter-efficient federated framework for streaming time series anomaly detection via lightweight adaptation. *TMC*, 2025.

[Nichol *et al.*, 2018] Alex Nichol, Joshua Achiam, and John Schulman. On first-order meta-learning algorithms. *arXiv preprint arXiv:1803.02999*, 2018.

[Rao *et al.*, 2022] Xuan Rao, Hao Wang, Liang Zhang, Jing Li, Shuo Shang, and Peng Han. Fogs: First-order gradient supervision with learning-based graph for traffic flow forecasting. In *31st International Joint Conference on Artificial Intelligence, IJCAI 2022*, pages 3926–3932. International Joint Conferences on Artificial Intelligence, 2022.

[Shao *et al.*, 2022] Zezhi Shao, Zhao Zhang, Fei Wang, and Yongjun Xu. Pre-training enhanced spatial-temporal graph neural network for multivariate time series forecasting. In *Proceedings of the 28th ACM SIGKDD conference on knowledge discovery and data mining*, pages 1567–1577, 2022.

[Shi *et al.*, 2023] Hongzhi Shi, Quanming Yao, and Yong Li. Learning to simulate crowd trajectories with graph networks. In *Proceedings of the ACM Web Conference 2023*, pages 4200–4209, 2023.

[Tang *et al.*, 2022] Yihong Tang, Ao Qu, Andy HF Chow, William HK Lam, Sze Chun Wong, and Wei Ma. Domain adversarial spatial-temporal network: A transferable framework for short-term traffic forecasting across cities. In *Proceedings of the 31st ACM International Conference on Information & Knowledge Management*, pages 1905–1915, 2022.

[Wang *et al.*, 2019] Leye Wang, Xu Geng, Xiaojuan Ma, Feng Liu, and Qiang Yang. Cross-city transfer learning for deep spatio-temporal prediction. In *Proceedings of the 28th International Joint Conference on Artificial Intelligence*, pages 1893–1899, 2019.

[Wang *et al.*, 2020] Senzhang Wang, Jiannong Cao, and S Yu Philip. Deep learning for spatio-temporal data mining: A survey. *IEEE transactions on knowledge and data engineering*, 34(8):3681–3700, 2020.

[Woo *et al.*, 2022] Gerald Woo, Chenghao Liu, Doyen Sahoo, Akshat Kumar, and Steven Hoi. Cost: Contrastive learning of disentangled seasonal-trend representations for time series forecasting. *arXiv preprint arXiv:2202.01575*, 2022.

[Wu *et al.*, 2019] Zonghan Wu, Shirui Pan, Guodong Long, Jing Jiang, and Chengqi Zhang. Graph wavenet for deep spatial-temporal graph modeling. In *Proceedings of the 28th International Joint Conference on Artificial Intelligence*, pages 1907–1913, 2019.

[Wu *et al.*, 2021a] Haixu Wu, Jiehui Xu, Jianmin Wang, and Mingsheng Long. Autoformer: Decomposition transformers with auto-correlation for long-term series forecasting. *Advances in neural information processing systems*, 34:22419–22430, 2021.

[Wu *et al.*, 2021b] Yuankai Wu, Dingyi Zhuang, Aurelie Labbe, and Lijun Sun. Inductive graph neural networks for spatiotemporal kriging. In *Proceedings of the AAAI Conference on Artificial Intelligence*, volume 35, pages 4478–4485, 2021.

[Wu *et al.*, 2021c] Yuankai Wu, Dingyi Zhuang, Mengying Lei, Aurelie Labbe, and Lijun Sun. Spatial aggregation and temporal convolution networks for real-time kriging. *arXiv preprint arXiv:2109.12144*, 2021.

[Yuan *et al.*, 2024] Yuan Yuan, Chenyang Shao, Jingtao Ding, Depeng Jin, and Yong Li. Spatio-temporal few-shot learning via diffusive neural network generation. In *The Twelfth International Conference on Learning Representations*, 2024.

[Zhang *et al.*, 2022] Xiang Zhang, Ziyuan Zhao, Theodoros Tsiligkaridis, and Marinka Zitnik. Self-supervised contrastive pre-training for time series via time-frequency consistency. *Advances in Neural Information Processing Systems*, 35:3988–4003, 2022.

[Zhang *et al.*, 2023] Zijian Zhang, Xiangyu Zhao, Hao Miao, Chunxu Zhang, Hongwei Zhao, and Junbo Zhang. Autostl: Automated spatio-temporal multi-task learning. In *Proceedings of the AAAI Conference on Artificial Intelligence*, volume 37, pages 4902–4910, 2023.

[Zhang *et al.*, 2024] Yudong Zhang, Xu Wang, Pengkun Wang, Binwu Wang, Zhengyang Zhou, and Yang Wang. Modeling spatio-temporal mobility across data silos via

personalized federated learning. *IEEE Transactions on Mobile Computing*, 23(12):15289–15306, 2024.

[Zhang *et al.*, 2025a] Yudong Zhang, Xu Wang, Xuan Yu, Zhaoyang Sun, Kai Wang, and Yang Wang. Drawing informative gradients from sources: A one-stage transfer learning framework for cross-city spatiotemporal forecasting. In *Proceedings of the AAAI Conference on Artificial Intelligence*, volume 39, pages 1147–1155, 2025.

[Zhang *et al.*, 2025b] Yudong Zhang, Xu Wang, Xuan Yu, Kuo Yang, Zhengyang Zhou, and Yang Wang. Fedstg: Breaking through spatio-temporal data silos with federated graph learning. In *Companion Proceedings of the ACM on Web Conference 2025*, pages 1534–1538, 2025.

[Zhang *et al.*, 2025c] Yudong Zhang, Xu Wang, Xuan Yu, Zhengyang Zhou, Xing Xu, Lei Bai, and Yang Wang. Diffode: Neural ode with differentiable hidden state for irregular time series analysis. In *2025 IEEE 41st International Conference on Data Engineering (ICDE)*, pages 2107–2120. IEEE Computer Society, 2025.

[Zheng *et al.*, 2023] Chuanpan Zheng, Xiaoliang Fan, Cheng Wang, Jianzhong Qi, Chaochao Chen, and Longbiao Chen. Increase: Inductive graph representation learning for spatio-temporal kriging. In *Proceedings of the ACM Web Conference 2023*, pages 673–683, 2023.

[Zhuang *et al.*, 2020] Fuzhen Zhuang, Zhiyuan Qi, Keyu Duan, Dongbo Xi, Yongchun Zhu, Hengshu Zhu, Hui Xiong, and Qing He. A comprehensive survey on transfer learning. *Proceedings of the IEEE*, 109(1):43–76, 2020.